glected. Since the diameter was much larger than the boundary-layer thickness, the flow was numerically treated as two-dimensional. The inflow profile was constructed from the $x = 115$ cm data. The CAMMLE shear stress predictions at $x = 237$ cm (Fig. 1a, lines) were slightly lower than the data; however, the model appeared to capture the trends of the turbulent flow physics. The CAMMLE model produced the best agreement with Mach number data (Fig. 2b). The Baldwin-Lomax, Prandtl, and k-ε models produced relatively poor results.

The second test case consisted of a hypersonic Mach 20 helium boundary layer.[13] Since the tunnel diameter was large compared with the wall boundary-layer thickness, the flow was treated as two dimensional in the numerical solutions. The inflow profile was constructed from the $x = 79$ in. data. The CAMMLE model velocity predictions at $x = 139$ in. (Fig. 3) are in excellent agreement with the data. The Baldwin-Lomax, Prandtl mixing length, and k-ε models were unsuccessful in predicting the "full" hypersonic velocity profile.

The last test case was a high-speed free mixing layer.[8] The numerical shear stress profiles at $x/H = 15$ (Fig. 2a) are reasonably predicted, again capturing the compressible turbulent flow trends. The CAMMLE model Mach number profile (Fig. 2b) is in good agreement with the data except near the outer edge of the layer. It is suspected that the effects of intermittency may have been important.

To assess the effects of the compressible terms, the Situ-Schetz[2] and Prandtl solutions were generated with the mixing lengths fixed to the values predicted by the CAMMLE model. The CAMMLE and Prandtl model results both agreed fairly well with the data. The Situ-Schetz formulation[2] significantly overpredicted the shear layer spreading. This result seemed problematical at first, since the Situ-Schetz model shear stress formulation is identical to that of the CAMMLE model. Hence, accounting for the compressible turbulence in all of the conservation equations with the CAMMLE model produced the improved prediction of the shear layer spreading. This is an important result since practically all modern techniques[4] require some sort of artificial "fix" to predict the correct spreading.

Conclusions

The effects of numerically including the compressible apparent mass terms in all of the conservation equations were assessed. A straightforward gradient transport analysis was applied to model the additional apparent mass term. This new formulation was incorporated into a modern Navier-Stokes computational fluid dynamics code. The new model as well as other popular models of varying complexity were numerically tested against experimental data. The new model produced significantly improved results. Hence, the numerical results reinforced the experimental conclusion that compressible turbulence terms are important for hypersonic wall boundary layers and high-density gradient flows. Finally, the numerical simplicity of the CAMMLE model may provide an engineering use for cases where higher-order models are not numerically applicable.

References

[1]Liou, W., and Shih, T., "On the Basic Equations for the Second-Order Modeling of Compressible Turbulence," NASA TM 105277, Oct. 1991.

[2]Situ, M., and Schetz, J., "New Mixing Length Model for Turbulent High Speed Flows," *AIAA Journal*, Vol. 29, No. 6, 1991, pp. 872, 873.

[3]Bushnell, D., and Beckwith, I., "Calculation of Nonequilibrium Hypersonic Boundary Layers and Comparisons with Experimental Data," *AIAA Journal*, Vol. 8, No. 8, 1970, pp. 1462–1469.

[4]Wilcox, D. C., "Dilatation-Dissipation Corrections for Advanced Turbulence Models," *AIAA Journal*, Vol. 30, No. 11, 1992, pp. 2639–2646.

[5]Mikulla, V., and Horstman, C., "Turbulent Stress Measurements in a Nonadiabatic Hypersonic Boundary Layer," *AIAA Journal*, Vol. 15, No. 12, 1975, pp. 1607–1613.

[6]Horstman, C. C., and Owen, F. K., "Turbulent Properties of a Compressible Boundary Layer," *AIAA Journal*, Vol. 10, No. 11, 1972, pp. 1418–1424.

[7]Owen, F., Horstman, C., and Kussoy, M., "Mean and Fluctuating Measurements of a Fully-Developed, Nonadiabatic, Hypersonic Boundary Layer," *Journal of Fluid Mechanics*, Vol. 70, Pt. 2, 1975, pp. 393–413.

[8]Bowersox, R., and Schetz, J., "Compressible Turbulence Measurements in a High-Speed High Reynolds Number Mixing Layer," AIAA Paper 93-0660, Jan. 1993.

[9]Bradshaw, P., "Compressibility Effects on Free Shear Layers," *The 1980-81 AFOSR-HTM Stanford Conference on Complex Turbulent Flows: Comparison of Computation and Experiment*, Vol. I, Stanford University Press, Stanford, CA, 1981, pp. 364–368.

[10]Schetz, J. A., *Boundary Layer Analysis*, Prentice-Hall, Englewood Cliffs, NJ, 1993.

[11]Li, T., and Nagamatsu, H., "Effects of Density Fluctuations on the Turbulent Skin Friction of an Insulated Flat Plate at High Supersonic Speeds," *Journal of the Aeronautical Sciences*, Vol. 18, No. 10, 1951, pp. 696, 697.

[12]Roe, P. L., "Approximate Riemann Solvers, Parameter Vectors, and Difference Schemes," *Journal of Computational Physics*, Vol. 43, No. 2, 1981, pp. 357–372.

[13]Fischer, M. C., Maddalon, D. V., Weinstein, L. M., and Wagner, R. D., "Boundary-Layer Pitot and Hot-Wire Surveys at $M_\infty \approx 20$," *AIAA Journal*, Vol. 9, No. 5, 1971, pp. 826–834.

Penetration and Mixing of Gas Jets in Supersonic Cross Flow

F. S. Billig* and J. A. Schetz†
Johns Hopkins University, Laurel, Maryland 20723

Introduction

THE flowfield resulting from transverse injection of a gas jet from a wall into a supersonic crossflow is of interest in a number of practical applications. In all of these, there is a need for an analysis that predicts the gross features of the flow with reliable accuracy at a reasonable computational cost. This led us to undertake an update of the simplified analysis JETPEN[1] developed earlier. The requirements were to permit treatment of injection at angles other than 90 deg and to include turbulent mixing into the plume after the Mach disk.

Analysis

JETPEN used the "effective back pressure" concept[2] that relates the behavior of the jet as it exits into a lower pressure supersonic crossflow to the well-documented case of an underexpanded jet into a quiescent fluid by a model for the average pressure in the surroundings defined as the effective back pressure p_{eb}. In the earlier work, the simple models $p_{eb} \approx 0.8\,p'_a \approx 2/3\,p'_{ta}$ were used, but these were developed for 90-deg injection. Here, the approach has been extended to more general cases. We will shortly introduce a correlation for the angle of the jet at the Mach disk δ_1, and the injection angle is δ_j. The effective back pressure is now modeled as an average of the static pressure in the approach flow p_a and the Newtonian impact theory prediction for the pressure on bodies inclined at δ_1 and δ_j, $p_{\delta 1}$ and $p_{\delta j}$, as $p_{eb} = (p_{\delta 1} + p_{\delta j} + 2p_a)/4$. The correlation for δ_1 used here is

$$\delta_1 = \delta_j - \left(\frac{q_a}{q_j}\right)^{1/4} \frac{180}{\pi} \sin(\delta_j) \tag{1}$$

The centerline trajectory of the jet to the Mach disk is taken as a parabola with δ_1 as the angle at the Mach disk. Also, we now choose to correlate the arc length along the trajectory to the Mach disk s rather than the vertical height of the Mach disk y_1 used before. The relation adopted is

Presented as Paper 92-5061 at the AIAA 4th International Aerospace Planes Conference, Orlando, FL, Dec. 1–4, 1992; received Jan. 25, 1993; revision received Feb. 2, 1994; accepted for publication Feb. 5, 1994.

*Chief Scientist, Aeronautics Department, Applied Physics Laboratory. Fellow AIAA.

†Consultant, Applied Physics Laboratory. Fellow AIAA.

$$\frac{s}{d_j^*} = M_j^{1/4}\left(\frac{p_j^*}{P_{eb}}\right)^{1/2} \tag{2}$$

As before, the conditions after the Mach disk are calculated as one-dimensional averages. The flow to the Mach disk is assumed isentropic and mixing is neglected. The area at the Mach disk is correlated as in Ref. 1. With all of this and continuity, the one-dimensional Mach number after the Mach disk can be determined from the same relation as earlier.[1]

With one exception, this completes the modeling of the flow to just after the Mach disk. For low injection angles, the radius at the Mach disk $d_2/2$ is often less than the height to the center of the Mach disk y_1. Obviously, that cannot be. We still use the same area, but now the plume cross section is taken to be a circle with a segment removed to represent the plume resting on the wall. The center of the circle is at y_1, but the radius must be increased to retain the same total area.

In JETPEN, there was a region 2 where the pressure relaxed from p_{eb} after the Mach disk to p_a. Then there was a region 3 where the plume turned back to the axial direction at constant pressure. The region downstream of the Mach disk is now viewed as a single flow module, and the equations of motion are solved numerically marching downstream with turbulent mixing of main stream fluid into the plume modeled by an entrainment relation.

The equations of motion to be solved in the region downstream of the Mach disk are continuity, normal momentum, streamwise momentum, and species and energy conservation. In these equations, we must model the entrainment function E^* and the average static pressure in the plume $p_{ave}(s)$.

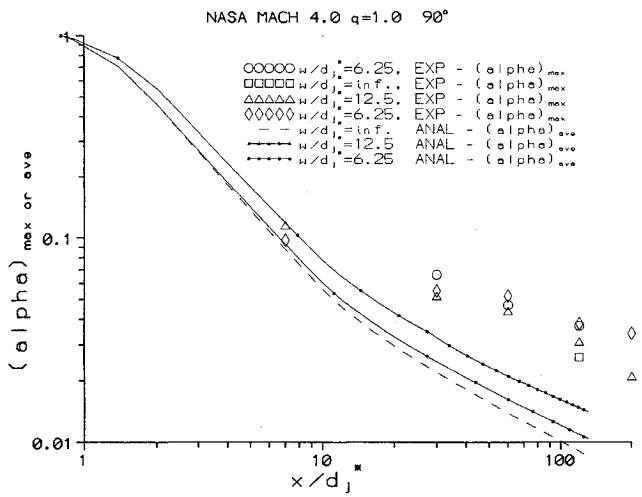

Fig. 1 Comparison of predictions and data for the experiments of Refs. 5 and 6 with $M_a = 4.0$ and $M_j = 1.0$.

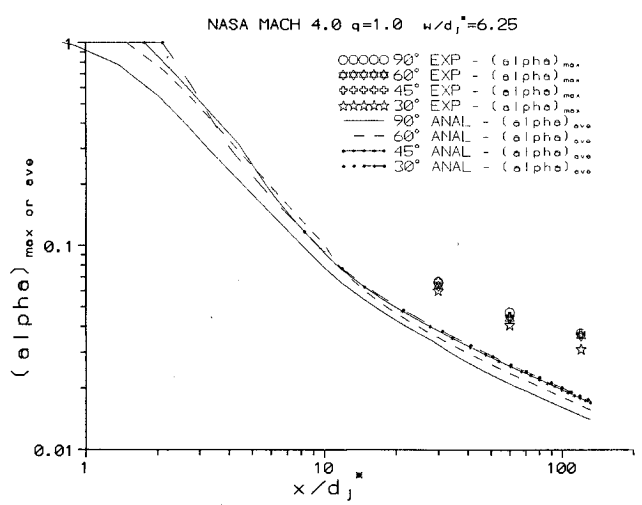

Fig. 2 Comparison of predictions and data for the experiments of Ref. 6 at various injection angles with $M_a = 4.0$ and $M_j = 1.0$.

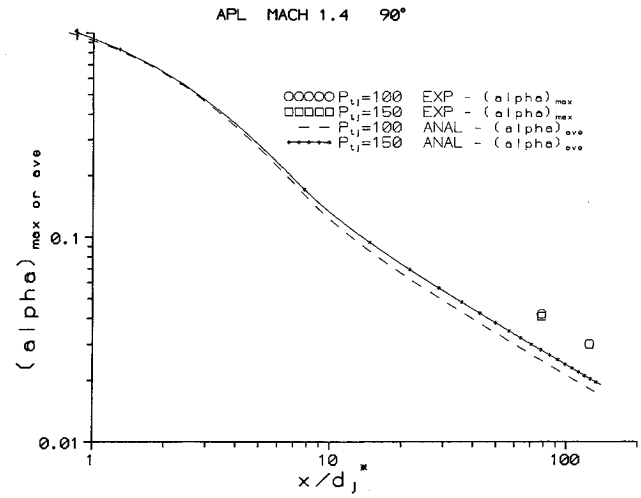

Fig. 3 Comparison of predictions and data for the experiments of Ref. 7 at $M_a = 1.4$.

The entrainment model is an extension of that in Ref. 3 for low-speed flows. In that work, the relation used was determined by correlating the limited data available in the range $0 \le s/d_j^* \le 10$ only for 90-deg injection and $4 < U_j/U_a < 8$. Here, we have made several changes to accommodate high-speed flows, the much larger range of s/d_j^*, lower values of U_j/U_a of interest, and angles other than 90 deg. First, the value of the velocity after the Mach disk is used rather than U_j. Second, the strong growth of E^* with s/d_j^* is stopped at $s/d_j^* = 10$. This is because the earlier database only covered that range and also because subsequent comparisons of predictions with data showed that such rapid growth was not supported by the data far downstream. Third, it was found necessary to increase the proportionality constant from 0.2 to 0.4. Thus, the current entrainment model is

$$E^* = \frac{0.4}{(U_2/U_a)^{0.6}}\left(\frac{s}{d_j^*}\right)^{1.37}, \qquad \frac{s}{d_j^*} \le 10 \tag{3}$$

Comparisons of predictions and experiment to be presented subsequently indicated that it was necessary to introduce an additional factor to account for the effects of angles other than 90 deg on entrainment. This lead us to adopt an empirical factor F_{ang}, that increased from a value of unity at 90 deg to 2.0 at 30 deg.

Two more items affecting entrainment had to be dealt with. The first involves the influence of jets on each other in a lateral array. The flow variables in this analysis are taken as constant across the jet plume at any axial station; this results in so-called top-hat profiles. In reality, the profiles are continuous, more or less Gaussian, profiles, and that results in greater lateral extent than implied by the top-hat profiles. The real profiles begin to interact sooner, as the jets spread and approach each other, than the assumed top-hat profiles imply. We have accounted for this by introducing a relation that reduces entrainment as the jets approach one another. The factor applied to the usual entrainment rule is

$$F_w = 0.5 + [(w/d_j^* - D/d_j^*) - 1.0]/18.0$$
$$(w/d_j^* - D/d_j^*) \le 10.0 \tag{4}$$

When the jets touch and beyond, the perimeter through which entrainment can occur is reduced, because the plume cross section is no longer a simple circle but rather a circle with segments clipped off by vertical straight lines on each side. The ratio of the reduced periphery compared to the perimeter of a circle with the same diameter F_P is applied as an additional factor to the entrainment rule.

The second effect on entrainment is similar except that it occurs when the jet plume rests on the wall. In that case, the bottom of the circular cross section is clipped off, and the periphery is again reduced.

The last item that had to be modeled is the average static pressure in the plume as a function of distance along the trajectory.

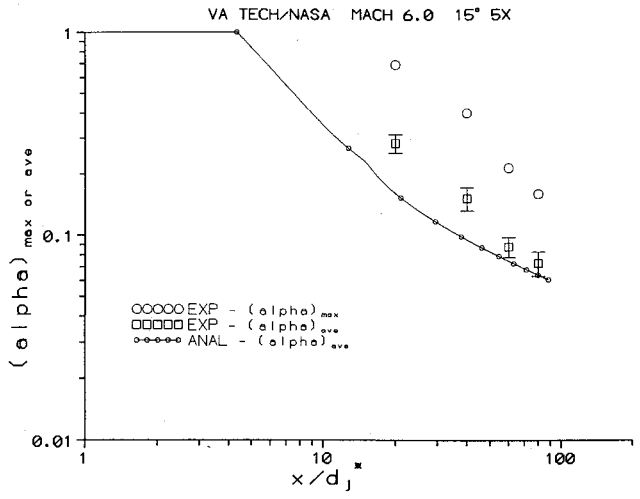

Fig. 4 Comparison of predictions and data for the experiments of Ref. 4 at $M_a = 6.0$ with $\delta_j = 15$ deg.

That is needed to calculate the density and thus the plume cross-sectional area but, most importantly, to calculate the pressure force in the streamwise momentum equation. The model adopted here assumes that Newtonian impact theory can be used to represent the effects of the inclination of the plume to the external flow and to relate the average pressure around the plume to that along the windward stagnation line.

Comparisons with Experiment

The comparisons will be based primarily on the decay of concentration of injectant fluid in the plume. The data is usually reported as the decay of the maximum concentration in the plume at any axial station, and the analysis predicts the one-dimensional average concentration in the plume. Seldom is enough information given to permit relating the maximum to the average concentration. The experiments in Ref. 4 did have enough information, and that implies $\alpha_{ave}/\alpha_{max} \approx 0.4$. Thus, the predictions of α_{ave} should be about 40% of the measured α_{max} at the same station.

We start using the $M_a = 4.0$ experiments reported in Refs. 5 and 6. These tests were all for H_2 injected into air at $M_j = 1.0$ and $\bar{q} = 1.0$. Consider the results shown in Fig. 1 looking first at the predictions and data for the single, isolated jets, i.e., $w/d_j^* = \infty$. As desired, the prediction for α_{ave} is roughly 40% of the measured α_{max}. The predictions also mimic the effects of the spacing w/d_j^* shown in the experiments quite well.

This same group of data can also be used to investigate the effects of injection angle. Predictions and data are given in Fig. 2 for injection angles from 30 to 90 deg, all with $w/d_j^* = 6.25$. The analysis predicts the effects of angle reasonably well.

The effects of a lower external stream Mach number can be probed using the $M_a = 1.4$ data of Ref. 7 which had He injection at $M_j = 1.0$. The results of measurements and the present analysis are plotted in Fig. 3. In this case, the ratio of α_{ave} predicted to α_{max} measured is closer to 60% than the 40% value obtained earlier.

The data of Ref. 4 allows testing the predictions of the analysis for a case with a low injection angle of 15 deg, albeit at a high Mach number of $M_a = 6.0$, with He injection at $M_j = 1.7$ and $w/d_j^* = 9.0$. The results are shown in Fig. 4. Here, the ratio of α_{ave} predicted to α_{max} measured is closer to the 40% value obtained earlier for the $M_a = 4.0$ cases. For this experiment, enough data was available to permit an approximate determination of α_{ave}, and those results are also included in Fig. 4 with 10% error bars. The mass flow of external stream fluid in the plume at three axial stations was measured, and those results can be used to approximately infer an entrainment rate. The experimental entrainment rate can then be compared to the entrainment rate predicted by the entrainment model to try and validate that model. The dimensionless entrainment rate obtained from the experiment in the region $60 \le x/d_j^* \le 80$ is 0.14, and the values from the analysis at $x/d_j^* = 60$ and 80 are 0.13 and 0.11, respectively.

References

[1]Billig, F. S., Orth, R. C., and Lasky, M., "A Unified Analysis of Gaseous Jet Penetration," *AIAA Journal*, Vol. 9, No. 6, 1971, pp. 1048–1058.

[2]Schetz, J. A., Hawkins, P. F., and Lehman, H., "Structure of Highly Underexpanded Transverse Jets in a Supersonic Stream," *AIAA Journal*, Vol. 5, No. 5, 1967, pp. 882–884.

[3]Campbell, J., and Schetz, J. A., "Analysis of Injection of a Heated Turbulent Jet into a Cross Flow," NASA TR R-413, 1973.

[4]Fuller, E. J., Mays, R. B., Thomas, R. H., and Schetz, J. A., "Mixing Studies of Helium in Air at High Supersonic Speeds," *AIAA Journal*, Vol. 30, No. 9, 1992, pp. 2234–2243.

[5]Rogers, R. C., "Mixing of Hydrogen Injected from Multiple Injectors Normal to a Supersonic Stream," NASA TN D-6476, 1971.

[6]McClinton, C. R., "The Effect of Injection Angle on the Interaction between Sonic Secondary Jets and a Supersonic Stream," NASA TN D-6659, 1972.

[7] Lee, R. E., private communication, Applied Physics Lab., Laurel, MD, Oct. 1992.

Impingement of Supersonic Jets on an Axisymmetric Deflector

J. K. Prasad‡ and R. C. Mehta§
Vikram Sarabhai Space Centre, Trivandrum 695022, India
and
A. K. Sreekanth¶
Indian Institute of Technology, Madras 600036, India

Nomenclature

De	= nozzle exit diameter
$\boldsymbol{F}, \boldsymbol{G}, \boldsymbol{H}$	= flux vector
M	= Mach number
M_e	= exit Mach number
P	= pressure
P_0	= total pressure
p_a	= ambient pressure
p_e	= exit pressure
p_s	= static pressure
r	= radial coordinate
T	= temperature
t	= time
$\boldsymbol{U}$	= vector of conserved variables
u, v	= axial and radial velocity, respectively
X_c	= distance measured from nozzle exit plane
x	= axial coordinate
ρ	= density

Introduction

THE phenomenon of supersonic jets and their interaction with solid surfaces is found in many engineering applications such as impingement of exhaust from launch vehicles during the liftoff phase, during stage separation of multistage rockets, and VTOL/STOL operation of aircraft, etc.

Many experiments have been carried out to study free jets.[1–4] A comprehensive experimental investigation of supersonic free jets was reported by Love et al.[5] Abdel-Fattah[6] has measured shock cell lengths for supersonic jets coming out of convergent-divergent nozzles in conjunction with schlieren pictures. Solution of parabolized Navier-Stokes equations using the shock capturing method

Received March 13, 1993; revision received Nov. 18, 1993; accepted for publication Dec. 30, 1993.

*Engineer, Aerothermal Test Facilities.
†Engineer, Aerodynamics Division. Senior Member AIAA.
‡Professor, Department of Aerospace Engineering.